Two-Color Spectroscopy of Colliding Ultracold Atoms

V. Bagnato,[a] L. Marcassa,[a] C. Tsao, Y. Wang, and J. Weiner[b]

Department of Chemistry and Biochemistry, University of Maryland, College Park, Maryland 20742

(Received 19 January 1993)

We present experimental results of two-color photoassociative ionization (TCPAI) spectroscopy in a magneto-optical trap. A probe light beam traces out the frequency (and intensity) dependence of TCPAI. By manipulating the intensities of the trap and repumper lasers we investigate the participation of different hyperfine ground-state levels and demonstrate the conditions under which molecular bound states figure in the collision intermediate.

PACS numbers: 33.80.−b, 34.50.−s

The study of two-body interactions between ultracold, trapped atoms is a new field of research revealing a rich array of dynamical phenomena and requiring a fresh examination of conventional ideas associated with heavy-particle collisions. The reduction of kinetic energy to below 1 mK ($E_{KE}=kT$) in the trapped atom ensemble renders the characteristic collision duration much longer than the excited-state spontaneous emission lifetime and permits exchange of photons between the optical field and colliding particles. Recent experiments [1] and theory [2–4] have begun to explore this novel physical domain.

Among the various collisional processes occurring in ultracold samples of trapped atoms, photoassociative ionization (PAI) [5] between pairs of sodium atoms has drawn particular attention because it is an ionizing inelastic process offering high detection efficiency and sensitivity. PAI begins when two ultracold ground-state atoms collide in the presence of a radiation field. The process occurs in two steps: (1) The system colliding on a ground state absorbs a photon and is promoted at long range to an attractive C_3/R^3 potential of an intermediate state. The two atoms begin to accelerate toward each other. (2) If this complex survives without spontaneous decay, it absorbs a second photon to a doubly excited molecular (Na_2^*) state which subsequently autoionizes to $Na_2^+ + e$ at short range.

Previous works [5] have investigated PAI for cases where the two photons were of the same color. Here we present experimental investigations of two-color PAI (TCPAI) where the color of one of the photons can be independently varied and where different hyperfine levels of the atomic ground state, $3s^2S_{1/2}(F=1)$ or $3s^2S_{1/2}(F=2)$, can be selected before starting the collision. This work constitutes the first two-color optical collision spectroscopy in an ultracold sample of trapped atoms.

Figure 1(a) shows a schematic of the experimental setup. Sodium vapor at a partial pressure corresponding to ~80 C, contained in a chamber at a base pressure lower than 10^{-8} torr, provides the atoms that load a magneto-optical trap (MOT) [6]. The trap is formed by three mutually orthogonal retro-reflected laser beams intersecting at the center of a quadrupole magnetic field generated by a pair of coils carrying opposite currents. The coils are located external to the chamber and produce a field gradient, in the trap region, $\simeq 20$ Gcm^{-1}. An Ar^+ ion pumped dye laser (laser 1) provides the laser beam for the trap. Before dividing into the three equal-intensity MOT beams the ring laser output passes through an electro-optic modulator (EOM) introducing sidebands at 1712 MHz to the red and blue of the central frequency. Power in each sideband is about 30% of the carrier. We operate the MOT in either of two modes: (1) the carrier frequency tuned near the trapping transition, ω_1 [$3^2S_{1/2}(F=2) \rightarrow 3^2P_{3/2}(F'=3)$], and the blue sideband

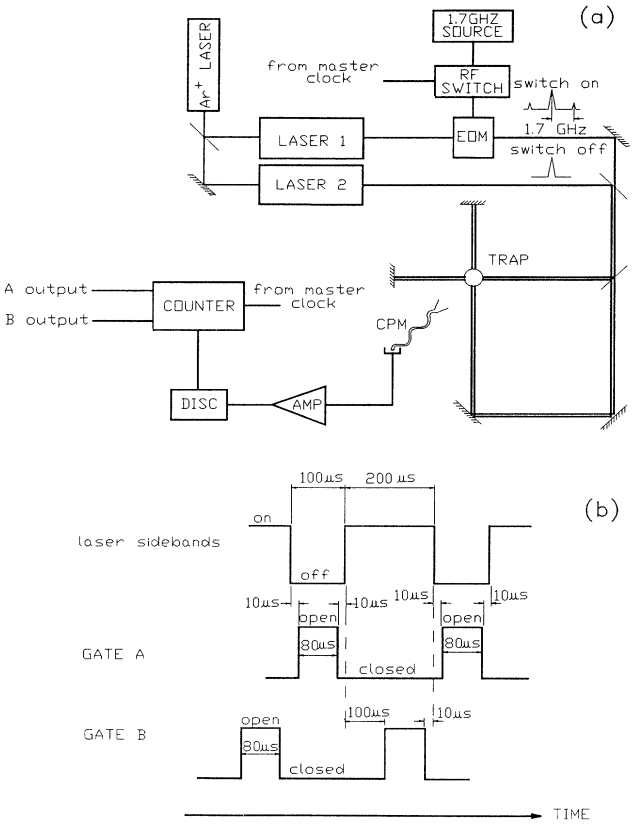

FIG. 1. (a) Schematic diagram of the experimental setup. One laser beam (laser 1) passing through an EOM is used for the MOT, while a probe laser (laser 2) scans. Ions are collected by a channeltron particle multiplier and counted. (b) Timing sequence for counting ions in gates *A* and *B* of the counter, synchronized with periods on-off of the laser sidebands.

positioned near the "repumper" transition, ω_2 [$3^2S_{1/2}(F=1) \rightarrow 3^2P_{3/2}(F'=2)$]; or (2) the red sideband tuned near ω_1 and the carrier close to ω_2. Mode (1) strongly drives the trapping transition, the usual arrangement, while mode (2) distributes ~63% of the available power to the repumper. The rf radiation exciting the EOM passes through a fast switch which turns on or off the sideband frequencies as desired. Focusing optics external to the MOT chamber capture a fraction of the trap fluorescence and image it onto a calibrated photomultiplier tube (PMT). This fluorescence monitors the number of atoms in the trap to insure stability as the spectroscopy experiments are carried out.

A second ring laser (laser 2) provides the probe beam (ω_p) introduced into the MOT as shown in Fig. 1(a). While the probe beam scans over a range of about 10 GHz, ions (Na_2^+) produced in the trap are collected by a channeltron particle multiplier (CPM) mounted about 28 mm from the trap. Charge pulses generated at the CPM pass through a fast amplifier-discriminator and are registered by a two-channel gated counter. A master clock synchronizes switching of the sideband modulation and counter gates for both channels (A and B) in the timing sequence shown in Fig. 1(b). We measure ion production rate as a function of frequency (and intensity) either with the MOT switch on or off. The sidebands of laser (1) cycle between periods of on for 200 μsec and off for the next 100 μsec. Gate A opens during the off cycle with a time delay of 10 μsec. Gate B opens during the on cycle with 100 μsec delay.

As the probe (laser 2) scans, a computer reads four independent channels: gate A, gate B, trap fluorescence, and a frequency reference for ω_p, derived from an atomic beam. The intensities of ω_1 and ω_2 are held constant (~240 and 80 mW cm^{-2}, respectively) while the intensity of ω_p can be independently varied up to 700 mW cm^{-2}. Unless otherwise specified, the probe laser intensity is maintained at its maximum value. We obtained two-color spectra under four different conditions.

First, with the sidebands switched on (ω_1, ω_2, and ω_p present) and with the MOT operating in mode (1), we measured the ion rate production at gate B as a function of ω_p. A typical spectrum, shown in Fig. 2(a), reveals two distinct features. As ω_p scans 300 ± 40 MHz to the blue side of ω_1, an asymmetric peak degraded to the blue appears. As ω_p continues to scan to higher frequency, we find a similar asymmetric peak near ω_2. In mode (1) the MOT operates with power distributed between the carrier and each of the sidebands in the ratio of 3:1. Measurements [7] on a MOT with conditions similar to mode (1) show that up to 50% of the ground-state atoms can be in the $F=1$ hyperfine level. Significant population of both hyperfine levels means that all three possible pairwise combinations contribute to collisional processes, and each of these possibilities corresponds to a different molecular potential asymptotic energy. For brevity we label these three molecular asymptotes as (1+1), (1+2), and (2+2). Singly excited molecular asymptotes are labeled (1+p), (2+p), and the double excited level, (p+p). The insets in Fig. 2(a) show the excitation routes responsible for the two features. The left-hand inset shows the paths responsible for the feature near ω_1. Two atoms approaching on the $F=2$ asymptote, (2+2), absorb a trap photon ω_1 and are promoted to C_3/R^2 attractive (2+p) potential. As the two atoms accelerate together, the probe laser ω_p induces a second, blueshifted absorption to (p+p) which autoionizes at short range. Collisions occurring on the (1+2) asymptote may also contribute to the feature around ω_1 by absorbing a repumper photon ω_2 as shown by the dashed line. The right-hand inset of Fig. 2(a) shows the two analogous routes responsible for the feature around ω_2, found simply by shifting all transitions by the ground-state hyperfine splitting.

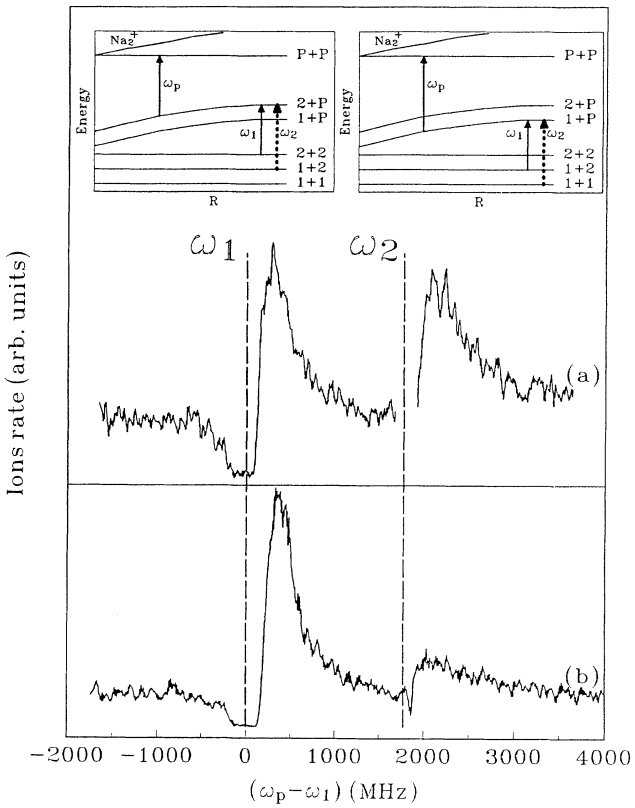

FIG. 2. (a) Ion spectrum as a function of probe laser frequency ω_p. Data obtained when the trapping frequency (ω_1) operates with 240 mW cm^{-2} and the repumper (ω_2) with 80 mW cm^{-2}. (b) Ion spectrum with light intensity on trapping and repumper transitions reversed. Insets represent proposed mechanisms for the observed features.

Second, in order to test these excitation mechanisms, we pumped more of the atomic population to the $F=2$ hyperfine level by running the MOT in mode (2), i.e., with the relative distribution of power between trap and repumper transitions reversed. The strong repumper reduces the atomic population of the $F=1$ level to only a

few percent [5], and the resulting spectrum is shown in Fig. 2(b). Suppression of the feature around ω_2 conforms to expectation since this feature requires $(1+1)$ or $(1+2)$ collisions. In contrast the feature around ω_1, relying on $(2+2)$ collisions, remains intact. Measurements confirm that both peaks of Fig. 2 depend linearly on probe laser intensity (ω_p) as expected.

Third, with the sidebands switched off (ω_p and ω_1 present) we measured ion rate production at gate A. Optical pumping transfers almost all population to the $F=1$ level within the 10 μsec delay between switching off the sidebands and opening the A channel [see Fig. 1(b)]. All observed TCPAI therefore must start from the (1,1) asymptote. The observed TCPAI spectrum for this case is presented in Fig. 3(a). The absence of the feature near ω_1 confirms that population on the $(2+2)$ and $(1+2)$ asymptotes is negligible. A new feature now appears near $2\omega_2$, consistent with the previously described two-step excitation mechanism [see right-hand inset in Fig. 3(a)]. In general form the profile of this new feature resembles those previously described—sharp onset with blue asymmetry—although a secondary peak $\sim$1400 MHz to the blue of the onset reproducibly appears for which we have no ready explanation. Other "structures" in the profile are irreproducible noise fluctuations. The intensity dependence of this feature with probe laser intensity is linear as expected. An unexpected peak also appears near ω_2 which cannot be explained with the familiar two-color, two-step mechanism. The properties of this feature are markedly different from that occurring at the corresponding frequency interval in Fig. 2(a). It is much narrower ($\sim$800 MHz) with a probe laser intensity dependence quadratic up to $\sim 350\ \mathrm{mW\,cm^{-2}}$ but exhibiting saturation at higher intensity. We propose a one-color (ω_p), two-photon mechanism as shown in the center inset in Fig. 3(a). As the atoms move toward each other, hyperfine mixing breaks down dipole selection rules in the region where C_3/R^3 becomes comparable to the hyperfine splitting. In this zone of internuclear distance $(1+p)$ and $(2+p)$ become strongly mixed. The initial photon couples the $(1+1)$ level to a hyperfine-mixed intermediate state at a first Condon point [where ω_p is resonant with the potential difference between $(1+1)$ and the mixed intermediate state]; the second photon then connects the intermediate state to the final $(p+p)$ level at a second Condon point. This mechanism is analogous to the interpretation of a recently reported [8] one-color PAI spectrum in which scattering flux starts on the $(1+2)$ rather than the $(1+1)$ level. The probe laser power in Ref. [8] is more intense than ω_p by more than a factor of 10 (3 W versus 250 mW), and our intentional optical pumping of $(1+1)$ together with a relatively weak ω_p explains why the dominant feature centered midway between ω_1 and ω_2 in Ref. [8] does not appear in Fig. 3. These two-photon features underscore the sensitivity to intensity and optical pumping and the importance of hyperfine interaction in ultracold collision dynamics [9].

Finally with the sidebands switched off (ω_p and ω_2 present) we again measured the ion spectrum at gate A. Optical pumping transfers almost all population to the $F=2$ level within the 10 μsec delay between switching off the sidebands and opening the A channel [see Fig. 1(a)]. All observed TCPAI therefore must start from the $(2+2)$ asymptote. For this case the TCPAI spectrum is

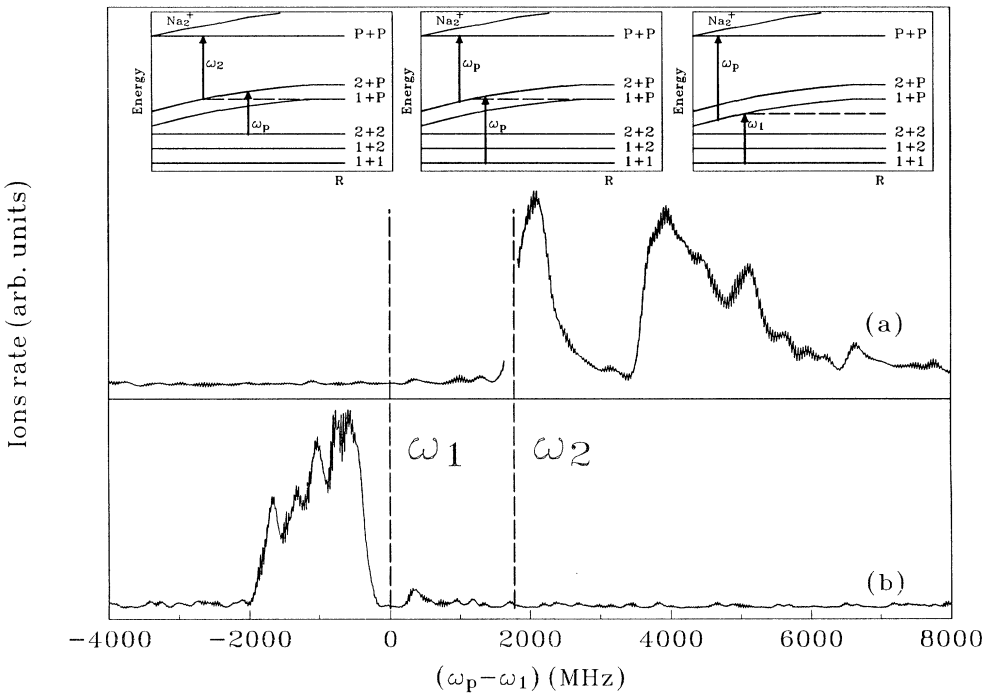

FIG. 3. (a) Spectrum of TCPAI obtained from gate A (sidebands off) of the counter. TCPAI spectrum excited from atom pairs in the $F=1$ hyperfine level. Trapping frequency (ω_1) and probe frequency (ω_p) present. Note the 300 MHz wide break in the spectrum centered around ω_2 due to MOT disruption by ω_p. (b) TCPAI spectrum excited from atom pairs in the $F=2$ hyperfine level. Repumper frequency (ω_2) and the probe frequency (ω_p) present. Insets represent proposed mechanisms for the observed features.

shown in Fig. 3(b). Only one peak near *and shifted to the red of* ω_1 is observed. The left-hand inset in Fig. 3(a) shows the proposed mechanism. In contrast to previous cases, the probe laser now provides the photon for the first step, taking the system from $(2+2) \rightarrow (2+p)$. The repumper at ω_2 supplies the second photon, and the transition $(2+p) \rightarrow (p+p)$ occurs at fixed internuclear distance. As ω_p scans from red to blue, the energy threshold for the process occurs at a position where $\omega_2+\omega_p$ equals the energy difference between the $(2+2)$ and $(p+p)$ asymptotes. Note that the first step involves free-bound transitions to vibration-rotation levels of the attractive intermediate. Indeed the spectrum exhibits five reproducible principal peaks spaced 250–350 MHz apart with evidence of substructure as well. This well-resolved free-bound-free collision spectrum is an example of high-resolution photoassociation spectroscopy made possible by the extremely narrow distribution of kinetic energy at ultracold temperatures [10].

The structureless asymmetric profiles shaded to the blue have been predicted by Gallagher [2] and bear the familiar form of the line-core and quasistatic wing often encountered in optical or "radiative" collisions [11,12]. In this semiclassical picture the profile maximum appears near the two Condon points where ω_1 (ω_2) and ω_p come into resonance with their respective difference potentials (see the insets in Figs. 2 and 3). The intensity falloff in the wing is due to two factors: decreasing pair distribution function with internuclear distance and a short time of passage through the second Condon point as ω_p tunes further into the blue. Comparison of the line shapes in Fig. 2(b) with the results of Ref. (2) shows good agreement with the form of the profile. Although one might expect that survival of the excited state against spontaneous emission would result in a blueshift, the peak of the feature appears shifted 200 MHz further to the blue than predicted. Band and Julienne [13] have also calculated the absorption profile for TCPAI by adapting quantum collisional close coupling to take explicit account of radiative dissipation to the vacuum modes of radiation field. Their preliminary results also achieve good agreement with the shape of the observed profile but do not account for the "anomalous" blueshift either.

The structure in the red-degraded feature of Fig. 3(b) should provide sufficient information to positively identify the intermediate state (or states) through which TCPAI takes place. According to the model of Heather and Julienne [3] (HJ) only gerade intermediate states play a significant role, and among these the 0_g^- long-range molecular state, first identified by Stwalley, Uang, and Pichler [14], would appear to be a leading candidate. In order to make a truly meaningful comparison, however, the HJ model must incorporate the hyperfine interaction in the adiabatic intermediate state manifold. Attack on this redoubtable problem is proceeding apace [9].

V.B. and L.M. acknowledge financial support from "Fundacao de Amparo a Pesquisa do Estado de Sao Paulo" (FAPESP), CNPq, and CAPES. J.W. acknowledges support from the National Science Foundation, the National Institute of Standards and Technology, and the Donors of the Petroleum Research Fund, administered by the American Chemical Society, for partial support of this research. The authors wish to thank Reginaldo Napolitano for numerical simulations of the population distribution of atoms and Paul Julienne for very helpful discussions.

[a]Permanent address: Instituto de Fisica e Quimica de Sao Carlos, Universidade de Sao Paulo, Caixa Postal 369, Sao Carlos, SP Brazil 13560.

[b]On leave at the Physics Division, National Science Foundation, 1800 G Street NW, Washington, DC 20550.

[1] At the present time total collisional trap loss and collisional ionization have been subject to experimental scrutiny. Recent references to collisional ionization are cited in V. Bagnato, L. Marcassa, Y. Wang, J. Weiner, P. S. Julienne, and Y. B. Band (to be published); also see F. Bardou, O. Emile, J.-M. Courty, C. I. Westbrook, and A. Aspect, Europhys. Lett. **20**, 681 (1992). Recent references to collisional trap loss are cited in L. Marcassa, V. Bagnato, Y. Wang, J. Weiner, P. S. Julienne, and Y. B. Band (to be published).

[2] A. Gallagher, Phys. Rev. A **44**, 4249 (1991).

[3] R. Heather and P. S. Julienne, Phys. Rev. Lett. **67**, 2139 (1991); Phys. Rev. A **47**, 1887 (1993).

[4] P. S. Julienne and Y. B. Band, Phys. Rev. A **46**, 330 (1992), and references cited therein.

[5] For the most recent studies of this process see, for example, M. Wagshul, K. Helmerson, P. Lett, S. Rolston, W. D. Phillips, R. Heather, and P. S. Julienne, Phys. Rev. Lett. **70**, 2074 (1993); V. Bagnato, L. Marcassa, Y. Wang, J. Weiner, P. S. Julienne, and Y. B. Band (to be published); P. Lett, P. Jessen, W. D. Phillips, S. Rolston, C. Westbrook, and P. Gould, Phys. Rev. Lett. **67**, 2139 (1991); P. Gould, P. Lett, P. S. Julienne, W. Phillips, H. Thorsheim, and J. Weiner, Phys. Rev. Lett. **60**, 788 (1988). For earlier studies see the review by J. Weiner, F. Masnou-Seeuws, and A. Giusti-Suzor, Adv. At. Mol. Opt. Phys. **26**, 209 (1989).

[6] E. Raab, M. Prentiss, A. Cable, S. Chu, and D. Pritchard, Phys. Rev. Lett. **59**, 263 (1987); C. Monroe, W. Swann, H. Robinson, and C. Wieman, Phys. Rev. Lett. **65**, 1571 (1990).

[7] D. Pritchard and W. Ketterle (private communication).

[8] M. Wagshul, K. Helmerson, P. Lett, S. Rolston, W. D. Phillips, R. Heather, and P. S. Julienne, Phys. Rev. Lett. **70**, 2074 (1993).

[9] P. S. Julienne and C. Williams (private communication).

[10] H. Thorsheim, J. Weiner, and P. S. Julienne, Phys. Rev. Lett. **58**, 2420 (1987).

[11] L. I. Gudzenko and S. I. Yakovlenko, Zh. Eksp. Teor. Fiz. **62**, 1686 (1972) [Sov. Phys. JETP **35**, 877 (1972)].

[12] A. Gallagher and T. Holstein, Phys. Rev. A **16**, 2413 (1977), and references cited therein.

[13] Y. Band and P. S. Julienne (private communication).

[14] W. C. Stwalley, Y-H. Uang, and G. Pichler, Phys. Rev. Lett. **41**, 1164 (1978).